JNeurosci
THE JOURNAL OF NEUROSCIENCE

Research Articles: Behavioral/Cognitive

Two Independent Frontal Midline Theta Oscillations During Conflict Detection and Adaptation in a Simon-type Manual Reaching Task

Thomas Töllner[1,2], Yijun Wang[3], Scott Makeig[4], Hermann J. Müller[1,5], Tzyy-Ping Jung[4] and Klaus Gramann[2,6]

[1]*Department of Experimental Psychology, LMU Munich, 80802 Munich, Germany*

[2]*Graduate School of Systemic Neurosciences, LMU Munich, 80802 Munich, Germany*

[3]*State Key Laboratory on Integrated Optoelectronics, Institute of Semiconductors, Chinese Academy of Sciences, Beijing 100083, China*

[4]*Swartz Center for Computational Neuroscience, Institute for Neural Computation, University of California, San Diego, La Jolla, CA 92093, USA*

[5]*Department of Psychological Sciences, Birkbeck College, University of London, London, WC1E 7HX, Great Britain*

[6]*Department of Biological Psychology and Neuroergonomics, TU Berlin, 10587 Berlin, Germany,*

DOI: 10.1523/JNEUROSCI.1752-16.2017

Received: 1 June 2016

Revised: 14 January 2017

Accepted: 23 January 2017

Published: 30 January 2017

Author contributions: T.T., Y.W., H.J.M., and K.G. designed research; T.T. and K.G. performed research; T.T. and Y.W. analyzed data; T.T., Y.W., S.M., H.J.M., T.-P.J., and K.G. wrote the paper.

The authors would like to thank Mike X. Cohen and two anonymous reviewers for their helpful comments on an earlier version of this manuscript. The authors are grateful to Andre Vankov for technical assistance, and gratefully acknowledge to SM the gift from The Swartz Foundation (Old Field, NY) that made possible our collaboration.

Correspondence should be addressed to Address for correspondence: Dr. Thomas Töllner, Email: thomas.toellner@psy.lmu.de, Postal address: Department of Experimental Psychology & Graduate School of Systemic Neurosciences, LMU Munich, Leopoldstrasse 13, D-80802 Munich

Cite as: J. Neurosci ; 10.1523/JNEUROSCI.1752-16.2017

Behavioral/Cognitive

Two Independent Frontal Midline Theta Oscillations During Conflict Detection and Adaptation in a Simon-type Manual Reaching Task

Thomas Töllner[1,2*], Yijun Wang[3*], Scott Makeig[4], Hermann J. Müller[1,5], Tzyy-Ping Jung[4]. and Klaus Gramann[2,6]

[1]Department of Experimental Psychology, LMU Munich, 80802 Munich, Germany, [2]Graduate School of Systemic Neurosciences, LMU Munich, 80802 Munich, Germany, [3]State Key Laboratory on Integrated Optoelectronics, Institute of Semiconductors, Chinese Academy of Sciences, Beijing 100083, China, [4]Swartz Center for Computational Neuroscience, Institute for Neural Computation, University of California, San Diego, La Jolla, CA 92093, USA, [5]Department of Psychological Sciences, Birkbeck College, University of London, London, WC1E 7HX, Great Britain, [6]Department of Biological Psychology and Neuroergonomics, TU Berlin, 10587 Berlin, Germany, [*]Equal contribution: T.T. & Y.W.

Keywords: Cognitive Control | Conflict Processing | Independent Component Analysis

Characters: max. 60 000 [incl. abstract, references, figure legends]

Address for correspondence:

Dr. Thomas Töllner

Email: thomas.toellner@psy.lmu.de

Postal address: Department of Experimental Psychology & Graduate School of Systemic Neurosciences, LMU Munich, Leopoldstrasse 13, D-80802 Munich

Abstract

One of the most firmly established factors determining the speed of human behavioral responses towards action-critical stimuli is the spatial correspondence between the stimulus and response locations. If both locations match, the time taken for response production is markedly reduced relative to when they mismatch—a phenomenon called Simon effect. While there is a consensus that this stimulus-response (S–R) conflict is associated with brief (4–7 Hz) frontal midline theta (fmθ) complexes generated in medial frontal cortex (MFC), it remains controversial (i) whether there are multiple, simultaneously active theta generator areas in the MFC that commonly give rise to conflict-related fmθ complexes; and if so, (ii) whether they are all related to the resolution of conflicting task information. Here, we combined mental chronometry with high-density electroencephalographic measures during a Simon-type manual reaching task and used independent component analysis and time-frequency domain statistics on source level activities to model fmθ sources. During target processing, our results revealed two independent fmθ generators simultaneously active in or near anterior cingulate cortex, only one of them reflecting the correspondence between current and previous S–R locations. However, this fmθ response is not exclusively linked to conflict but also to other, conflict-independent processes associated with response slowing. These results paint a detailed picture regarding the oscillatory correlates of conflict processing in Simon tasks, and challenge the prevalent notion that fmθ complexes induced by conflicting task information represent a unitary phenomenon related to cognitive control, which governs conflict processing across various types of response-override tasks.

Significance Statement

Humans constantly monitor their environment for and adjust their cognitive control settings in response to conflicts—an ability that arguably paves the way for survival in ever-changing situations. Anterior cingulate-generated frontal midline theta (fmθ) complexes have been hypothesized to play a role in this conflict-monitoring function. However, it remains a point of contention whether fmθ complexes govern conflict processing in a unitary, paradigm-nonspecific manner. Here, we identified two independent fmθ oscillations triggered during a Simon-type task, only one of them reflecting current and previous conflicts. Importantly, this signal differed in various respects (cortical origin, intertrial history) from fmθ phenomena in other response-override tasks, challenging the prevalent notion of conflict-induced fmθ as a unitary phenomenon associated with the resolution of conflict.

Introduction

It is well established that human behavioral responses are slower when the appearance of a response-imperative stimulus is spatially incongruent with its associated response (e.g., a left stimulus prompting a right-hand, rather than a left-hand, response). This reaction time (RT) difference—often referred to as "Simon effect" (Simon and Small Jr, 1969)—is independent of the sensory modality of the stimulus and depends on the spatial location of the motor action rather than the actual effector (e.g., left vs. right hand) with which the action is executed (Simon, 1969; Wallace, 1971). Thus, theoretical accounts (Umiltà and Nicoletti, 1992; Hommel et al., 2004) generally agree that the Simon effect is driven by the *conflict* between representations that code the stimulus and, respectively, response locations. The degree of this conflict-related slowing is further determined by the recent history of spatial conflict (Gratton et al., 1992; Mayr et al., 2003; Ullsperger et al., 2005; Egner, 2007): incongruent responses are faster on a given trial when the preceding response was also incongruent. This "conflict-adaptation effect" (also referred to as "Gratton effect") suggests that encountering a conflict gives rise to an adjustment of internal system settings such that performance is facilitated on a subsequent conflict trial (Gratton et al., 1992; Ridderinkhof et al., 2004; Töllner et al., 2012a).

At the level of brain dynamics, there is mounting evidence that at least two frontal brain regions are involved in behavioral adjustments following a response conflict in the Simon task. Kerns (2006) showed that conflict-related hemodynamic activity in anterior cingulate cortex (ACC) is related to increased prefrontal cortex (PFC) activity, which, in turn, is associated with improved behavioral responses on the next trial. Following the conflict-monitoring hypothesis (Botvinick et al., 2004), Kerns suggested that the ACC becomes activated whenever a conflict is detected, and this activation is then projected to other brain areas (including the PFC) involved in the pro-active minimization of potential conflicts on subsequent trials.

Complementing these hemodynamic findings, recent electroencephalographic (EEG)

investigations have provided insights into the *spectro-temporal* brain dynamics that mediate conflict detection and adaptation in the classical Simon task (Cohen and Ridderinkhof, 2013; Gulbinaite et al., 2014) as well as in (cueing) variants of this task (Cavanagh et al., 2012; van Driel et al., 2015; Mückschel et al., 2016). The emerging picture suggests that the non-correspondence between stimulus (S) and response (R) locations is associated with brief medial frontal cortex (MFC)-generated theta complexes. In more detail, trials with incongruent S–R locations give rise to stronger frontal midline theta (fmθ) complexes than trials with congruent locations (Cavanagh et al., 2012), with conflict-induced fmθ complexes being reduced when participants had processed a conflict on the preceding trial (Cohen and Ridderinkhof, 2013). These and other findings led to the prominent proposal that such fmθ complexes are associated with a brain process that mediates conflict processing (Nigbur et al., 2011). At variance with this view, others have argued that conflict-related theta modulations, rather than reflecting processing of conflict *per se*, are attributable to more general "time-on-task" processes (Scherbaum and Dshemuchadse, 2013). That is, the changes in the oscillatory EEG pattern may simply reflect changes in RT performance.

The present study was designed to provide a more detailed picture as to (i) whether there are multiple, concurrently active theta generators in the MFC, and if so, (ii) whether they are all related to S–R conflict. For example, it is conceivable that separable fmθ-associated processes (e.g., conflict detection, adaptation, conflict-unrelated processes) arise from functionally and physiologically distinct theta activities, not easily detectable by conventional analyses of scalp channel signals. Alternatively, different conflict-related and -unrelated processes may drive one-and-the-same fmθ complex. To decide between these alternatives, we recorded high-density EEG during a Simon-type manual reaching task and used independent component analysis (ICA) (Makeig et al., 1996) to decompose statistically independent source processes whose spatial origins could then be studied using equivalent dipole modeling (Makeig et al., 2002).

Materials and Methods

Participants. Fourteen healthy adults recruited from the University of California San Diego took part in this study; data from two participants had to be excluded because of excessive artifacts during EEG acquisition. The remaining twelve participants were between 20 to 30 (median 25) years of age; by chance, ten were male. They had all normal or corrected-to-normal vision, and none reported a history of neurological disorders. Each participant provided written informed consent prior to the start of the experiment. All experimental procedures were approved by the local Institutional Review Board in accord with the Code of Ethics of the World Medical Association (Declaration of Helsinki).

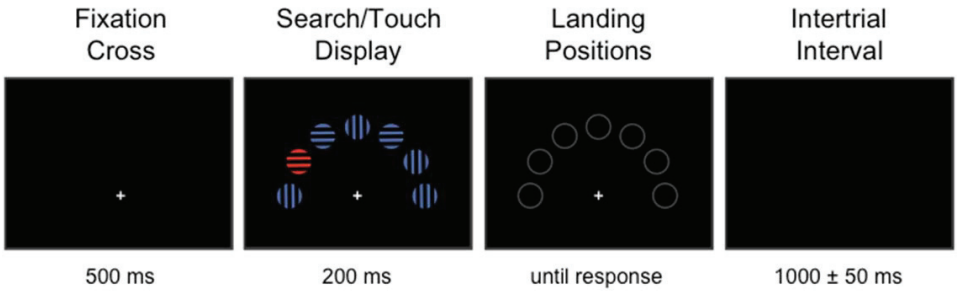

Figure 1. Sample trial sequence in the present Simon-type manual reaching task. The target was randomly defined by color (red) or shape (square), with the correct motor response (left vs. right hand) being defined—independently of the target-defining attribute (color vs. shape)—by the orientation of the stripes inside the target (vertical vs. horizontal). Target positions were selected randomly, on a trial-by-trial basis, from all but the central and the two outer positions.

Stimulus, Task, and Study Design. Visual displays consisted of seven colored shapes on a black background, which were arranged regularly on a semi-circle around a (central) white fixation cross at the screen bottom; the stimulus eccentricity was 6.0° of visual angle (Fig. 1). On each trial, a feature singleton target—randomly defined by color (red circles; CIE 0.213, 0.264, 68; radius: 2.4°) or shape (blue squares; CIE 0.389, 0.518, 68; 4.8° x 4.8°)—was presented together with six homogeneous distractor items (blue circles; CIE 0.389, 0.518, 68; radius: 2.4°). The position of the target was selected randomly from all but the central (upper)

and the two outer (left- and right-most) positions. Each stimulus outline contained a grating composed of three black bars (0.8° x 4.8°) separated by two gaps (0.6° x 4.8°), randomly oriented either vertically or horizontally.

Participants were seated comfortable in a dimly lit, sound-attenuated experimental booth. Visual displays were presented on a 21-inch computer touch screen monitor. Each experimental session consisted of 20 blocks of 60 trials each, yielding a total of 1200 trials. A trial started with a white central fixation cross displayed for 0.5 s, followed by the stimulus display presented for 0.2 s. Next, all stimuli were masked by "placeholders" (Fig. 1) until the participant's response or for a maximum period of 0.8 s. In case of a response error or if no response was issued within the maximum allowed RT window (1 s), the word **"**ERROR**"** was presented centrally for 1 s. In the interval to the next trial, participants were presented with a central white fixation cross for a randomly chosen duration of 0.95, 1, or 1.05 s. To initiate the trial, they had to press two customized keypad buttons mounted centrally on the lower frame of the touch-screen using both index fingers.

Participants were asked to maintain central eye fixation throughout all blocks and to perform, as fast and as accurately as possible, a visually guided manual reaching action. To dissociate perceptual from motor response selection for the planned inter-trial analyses, we employed a compound-search design (Töllner et al., 2008; Töllner et al., 2012b): participants had first to detect and localize the target (defined by a unique color or shape) before they could extract the information (the target's vertical vs. horizontal stripe orientation) that specified the required motor action: touching the target (location) on the (touch) screen using either their left- or their right-hand index finger, depending on the stripe orientation. Half the participants started to respond to vertical orientation with their left and to horizontal orientation with their right hand, and vice versa for the other half (the S–R mapping was reversed halfway through the experiment). Note that we used vertical versus horizontal orientation as response-critical attributes as these do not convey any lateralized information

that might have confounded the Simon effect (Hommel, 2011). To start a trial, participants had to (re-)position both index fingers on the keypad buttons (i.e., the starting positions), and trials were immediately aborted and counted as errors if both keypad buttons (rather than just one) were released during a trial. Before the start of the experiment, one block of practice (= 60 trials) was administered to familiarize participants with the S–R mapping (e.g., vertical/horizontal target orientation demanding a left-/right-hand response). After each block, participants received summary statistics feedback (mean RT and error rate).

Electroencephalographic recording and analysis. The EEG was digitized continuously at 512 Hz employing a 248-channel active electrode array (Active II, Biosemi, The Netherlands). Electrodes were mounted on an elastic cap, with exact locations measured individually using a 3-D ultrasound digitizer system (Polhemus, Inc.). Electrode impedances were kept below 20 kΩ. All offline EEG analyses were based on custom MATLAB (Mathworks) scripts, built on the open source EEGLAB toolbox (Delorme and Makeig, 2004). To start with, we inspected all raw data visually to identify and manually remove non-stereotypical noise. Next, we rejected all channels exhibiting excessive artifacts, defined as any signal exceeding ±1 mV, and channels with kurtosis larger than five standard deviations from the mean kurtosis across all channels. The EEG data were then high-pass filtered (0.1 Hz), re-referenced to average reference, and decomposed into temporally maximally independent source processes using adaptive mixture independent component analysis (AMICA) (Palmer et al., 2006; Palmer et al., 2008; Delorme et al., 2012)—which generalizes previously established infomax (Bell and Sejnowski, 1995; Makeig et al., 1996) and multiple mixture ICA approaches (Lee et al., 1999; Lewicki and Sejnowski, 2000), to dissociate scalp-recorded EEG signals into spatially static components that are statistically maximally independent. Of importance for the question at issue in the current study, ICA does not only dissociate brain from non-brain sources, but also other activities projecting to the scalp from multiple brain sources.

Electrocortical source analysis. For each of the independent component (IC) scalp topographies, a single-equivalent current dipole model was computed employing a boundary element head model (BEM) (Fuchs et al., 2002; Oostenveld and Oostendorp, 2002) as implemented in the DIPFIT plug-in of the EEGLAB toolbox. Co-registration of the electrode positions with the MNI (Montreal Neurological Institute; Quebec) brain template (representing an average MRI scan from 152 healthy adults; available at http://www.mni.mcgill.ca) was performed by aligning particular landmarks (nasion, inion, ears, and vertex) and, if required, rescaling and/or rotating the montage setting. Next, we selected ICs for further analysis only if their equivalent current dipoles were located within cortical gray matter; restated, we excluded all ICs with dipoles localized outside the brain (including those accounting for eye movement or muscle activity). In addition, we rejected any ICs from further analyses whose equivalent dipole model accounted for less than 85% of the variance of the IC scalp map (e.g., ICs with multifocal scalp maps not compatible with generation in a single cortical region).

IC clustering and statistics. Following ICA decomposition, the EEG data were epoched into 3-s segments, ranging from 1 s before to 2 s after stimulus onset. All remaining ICs were then clustered across all participants based on their spatial projections and measures of their event-related brain dynamics (Delorme and Makeig, 2004; Gramann et al., 2010)—including their equivalent dipole locations, scalp maps, mean log spectra, event-related potentials (ERPs), inter-trial coherences (ITCs), and event-related spectral perturbations (ERSPs) (Makeig, 1993)—applying a k-means approach. ICs more than three standard deviations distant from the cluster centroid were removed from each cluster. We then inspected all clusters to identify IC sets with a cluster mean scalp topography exhibiting a weight distribution with a maximum over fmθ areas (for theta band analysis; cf. Ishii et al., 1999; Buzsaki, 2006; Cohen et al., 2008).

ERSPs—our main measure of interest (see below)—were computed by transforming each IC time series into a spectrographic image. Frequency-specific event-related changes in spectral power were calculated across the frequency range 3 to 128 Hz using Morlet wavelet decomposition (as implemented in EEGLAB). Specifically, we used 3-cycle Morlet wavelets for the lowest frequency (3 Hz) and linearly increased the cycle number (per wavelet) to 25.6-cycle Morlet wavelets for the highest frequency (128 Hz) to balance the frequency/temporal-resolution trade-off. Spectrographic images for each trial were then averaged and converted to log power. Log power at each frequency in the pre-stimulus baseline period (-1 s to stimulus onset) was subtracted from the log spectrogram.

To statistically analyze both conflict detection and adaptation effects, all (left- and right-hand response) trials were first separated into "congruent" (i.e., left/right stimulus location requiring left/right motor action) and "incongruent" trial types (i.e., left/right stimulus location requiring right/left motor action). These two conditions were then further split as a function of previous—"congruent" versus "incongruent"—trial history, resulting in four experimental conditions (congruent-congruent, incongruent-congruent, congruent-incongruent, incongruent-incongruent). All behavioral (reaction times) and neural measures (ERSPs) were analyzed using separate repeated-measures ANOVAs with the factors 'Current S–R congruency' (congruent, incongruent) and 'Previous S–R congruency' (congruent, incongruent). Significant main effects and/or interactions were further verified by means of post-hoc comparisons (two-tailed paired t-tests). For spectro-temporal analyses, theta-band (4-7 Hz) ERSP values were extracted and analyzed for both stimulus-locked segments (from 0.5 s before to 1 s after stimulus onset) and response-locked segments (from 1 s before to 0.5 s after response onset) on the component cluster level.

Results

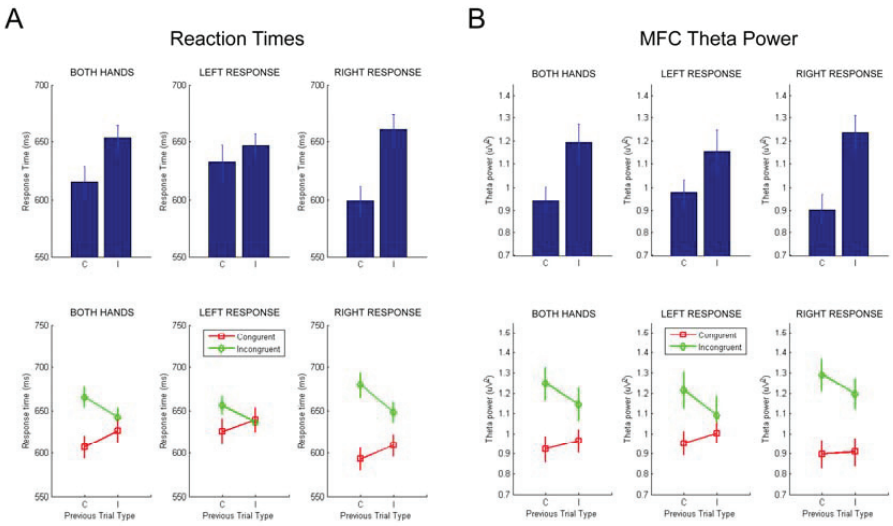

Figure 2. Conflict-related behavioral and neural responses averaged across hands, separately for left-hand and right-hand responses. **A**, Top panel: Differences in RTs between congruent (C; no-conflict) and incongruent (I; conflict) trials; bottom panel: RTs separately for congruent (red lines) and incongruent trials (green lines) as a function of the S–R compatibility on the previous trial. **B**, Top panel: Differences in MFC theta activations between congruent (no-conflict) and incongruent (conflict) trials; bottom panel: MFC theta activations separately for congruent (red lines) and incongruent trials (green lines) as a function of the previous S–R compatibility.

Behavioral data

Replicating the classical Simon task literature, RTs were robustly modulated by spatial S–R compatibility (Figure 2A, top panel): participants responded slower when the side of the motor action was spatially incongruent, as compared to congruent, with the side on which the target stimulus was presented (653.22 ± 42.06 ms vs. 615.63 ± 48.93 ms, $p < 0.001$). Importantly, the S–R compatibility effect interacted with the S–R compatibility on the previous trial ($F(1,13) = 165.25$, $p < 0.001$): responses were produced faster on incongruent trials (642.39 ± 42.03 ms vs. 665.61 ± 42.92 ms) and slower on congruent trials (625.99 ± 48.54 ms vs. 607.09 ± 49.25 ms) if participants had previously responded to an incongruent target (Fig. 2A, bottom panel). As further depicted in Figure 2A, the general RT pattern was

277 the same when calculating left- and right-hand responses separately. Participants exhibited
278 slightly more error-prone behavior on congruent (6.90 ± 1.88 % vs. 6.14 ± 1.73 %) and
279 incongruent trials (6.46 ± 1.31 % vs. 6.16 ± 2.21 %) when there was an S–R incompatibility
280 on the previous trial. However, none of the error-related differences reached statistical
281 significance (all p-values > 0.18).

282

283 *Frontal midline IC clusters*

284 In line with the central question at issue, and for the sake of brevity, we present results only
285 for those IC clusters whose centroids were located within cortical grey matter and whose
286 mean scalp topography exhibited a weight distribution maximal over frontal midline scalp
287 areas (from which fmθ effects are typically measured). Two clusters with centroids located in
288 or near dorsal anterior cingulate cortex (ACC) fulfilled these criteria. These clusters showed
289 functionally distinct EEG dynamics under different experimental conditions: the first cluster
290 comprised ICs from eight participants whose model equivalent dipoles were located in or near
291 medial prefrontal cortex (MPFC); the second cluster comprised ICs from ten participants
292 localized in or near the medial frontal cortex (MFC). Scalp projections of the ICs in each
293 cluster are depicted in Figure 3A. As can be seen from Figure 3B, equivalent dipoles for ICs
294 in the two theta clusters show distinctive distributions in MPFC and MFC areas, respectively.

295

296 *Frontal midline theta activity and conflict detection*

297 Figure 3C presents the spectrographic ERSP images for both the MPFC (left panel) and MFC
298 (right panel) IC clusters synchronized to the onset of the stimulus. ERSP analyses revealed
299 that both fmθ clusters produced clearly distinguishable brief enhancements in mean theta
300 power (4-7 Hz) for both congruent and incongruent S–R conditions. In addition to the theta
301 burst, the MPFC cluster selectively exhibited an event-related synchronization (ERS) in the

low beta frequency band (12–15 Hz), whereas the MFC cluster selectively exhibited an event-related desynchronization (ERD) in the mid-beta band (20–24 Hz). Most importantly, however, incompatibility between the S and R sides (i.e., the S–R conflict) was exclusively accompanied by event-related theta band activity changes in the MFC cluster. That is, when subtracting the congruent from the incongruent S–R condition, the only difference that remained was theta band activity in the MFC cluster (see Fig. 3C). This observation was statistically substantiated by stronger MFC theta bursts in the incongruent as compared to the congruent S–R conditions (1.19 μV^2 [± 0.25] vs. 0.94 μV^2 [± 0.19]; $p < 0.01$; see also top panel of Fig. 2B)—in line with the notion that heightened conflict processing goes along with stronger MFC activity (e.g., Kerns, 2006). The theta burst in the MPFC cluster, the beta ERS in the MPFC cluster, as well as the beta ERD in the MFC cluster, by contrast, occurred independently of S–R conflict—that is, there were no significant differences between congruent and incongruent conditions (all p-values > 0.14).

MFC theta activity and conflict adaptation

In the next step, we analyzed the theta band activity in the conflict-dependent MFC cluster as a function of preceding—congruent versus incongruent—trial history. This analysis revealed the theta band activity on the current trial being modulated by the S–R compatibility on the previous trial (bottom panel of Fig. 2B). Theta bursts triggered on incongruent trials were significantly reduced when participants had processed an incongruent, rather than a congruent, S–R condition in the preceding trial episode (1.14 μV^2 [± 0.25] vs. 1.24 μV^2 [± 0.25]; $p < 0.01$). By contrast, theta bursts on congruent trials were significantly enhanced when participants had processed an S–R conflict on the previous trial (0.96 μV^2 [± 0.18] vs. 0.92 μV^2 [± 0.19]; $p < 0.01$). As with the RT data, essentially the same interactive pattern was evident when plotting the MFC theta power separately for left- and right-hand responses (bottom panel of Fig. 2B). This set of findings is in line with the notion that, after having

328 encountered conflict, humans reactively adjust their internal system settings in order to
329 proactively prevent, or minimize, the costs associated with conflicts that potentially occur on
330 subsequent trials (Botvinick et al., 2001; Kerns, 2006).
331

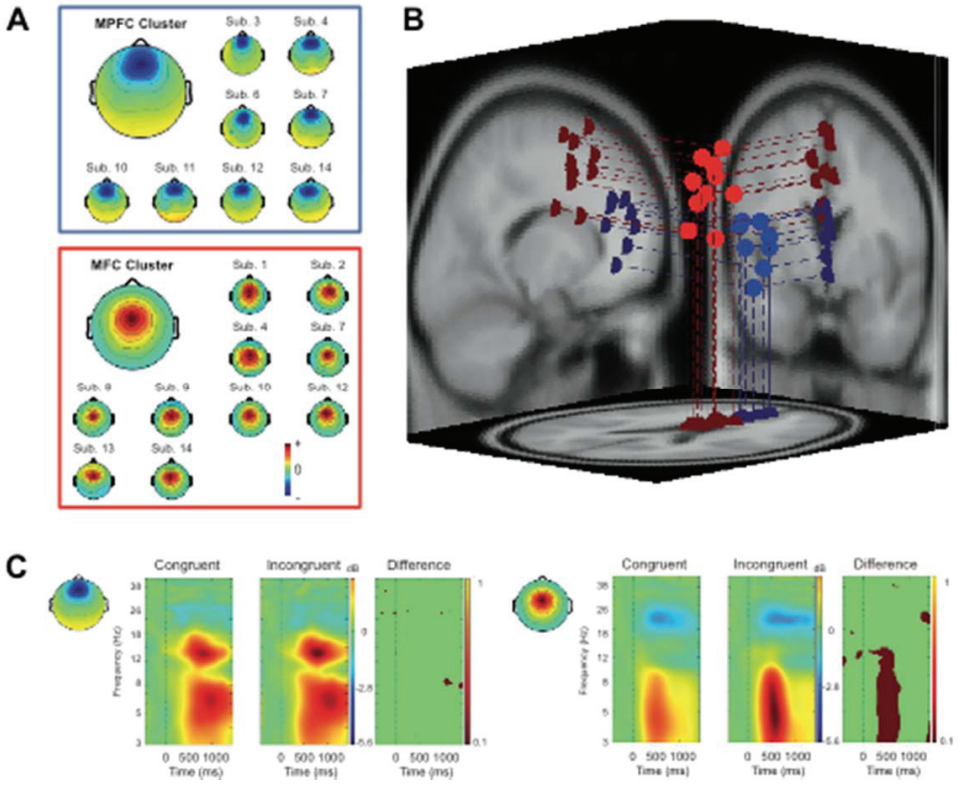

332

333 **Figure 3.** Two clusters of independent component (IC) EEG source processes with equivalent dipole centroids
334 in or near anterior cingulate cortex (ACC). **A**, (Larger maps) Mean scalp topographies for the medial prefrontal
335 cortex (MPFC, top) and medial frontal cortex (MFC, bottom) IC clusters. (Smaller maps) Topographies of their
336 individual ICs. Map sign orientation (red vs. blue) is arbitrary. **B**, Equivalent dipole locations of individual ICs in
337 the MPFC (blue spheres, lines) and MFC (red spheres, lines) IC clusters projected on horizontal, sagittal, and
338 coronal views of the standard MNI template brain. Cluster centroids of the equivalent dipole locations (not
339 shown) are MPFC, BA32, Talairach coordinates: x=1, y=38, z=11 (blue); MFC, BA32, Talairach coordinates:
340 x=0, y=9, z=39 (red). **C**, Cluster-mean event-related spectral perturbations time-locked to onset of stimuli
341 mandating spatially congruent and incongruent responses, respectively, for the MPFC (left panel) and MFC
342 (right panel) IC clusters. Significant ($p<0.01$ by two-tailed paired t-tests) incongruent-minus-congruent ERSP
343 differences between the two conditions are shown in dark red. Note the absence of an fmθ difference for the
344 MPFC cluster.

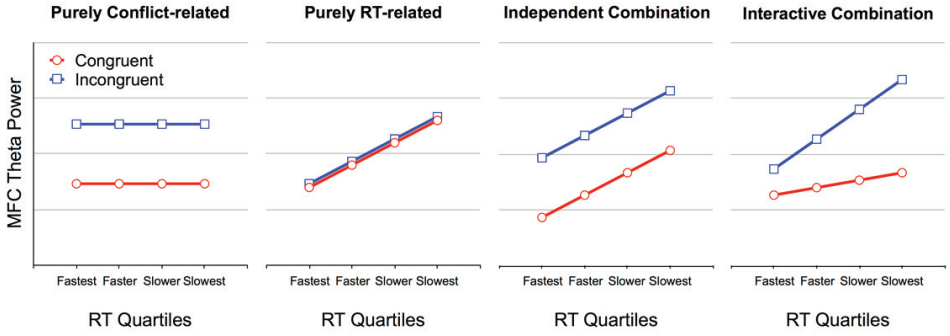

Figure 4. Hypothetical data patterns for MFC theta power. Left panels: Predicted MFC theta increases produced by a pure conflict-related versus a pure RT-related modulation. Right panels: Predicted MFC theta increases produced by a combination of both conflict- and RT-related modulations, determining MFC theta power either independently of one another or interactively. Note that in all hypothetical scenarios, each RT quartile is assumed to correspond to the same bounds for congruent (red lines) and incongruent trials (blue lines).

Dissociating conflict processing from general RT-related slowing in MFC theta power

However, one common difficulty in using RT paradigms to study EEG oscillations is that any change in the oscillatory pattern may be a direct correlate of a concurrent RT change. Applied to the present data, this implies that the increase in theta power for incongruent relative to congruent trials may not reflect the conflict between internal representations that code spatial S–R locations, respectively, but rather more general RT slowing or time-on-task processes (Scherbaum and Dshemuchadse, 2013). In other words, it remains unclear at this stage whether the MFC theta bursts in the present Simon-type task are due to (i) the conflict between S–R locations, (ii) more general processing demands associated with RT slowing, or (iii) a mixture of both. If MFC theta bursts reflect exclusively the S–R conflict, we should observe MFC theta being triggered more markedly for incongruent relative to congruent trials, without any RT modulation (Fig. 4, first panel). By contrast, if the MFC theta increase reflects exclusively RT-related processing demands, MFC theta power should increase gradually as RT increases, without any modulation by S–R compatibility (Fig. 4, second panel). If the MFC theta increase reflects both effects, however, we should observe MFC theta power being

triggered more strongly for incongruent relative to congruent trials, with further increases in trials with slow RTs. In the latter case, two scenarios are conceivable: The RT-related increase in MFC theta across different RT ranges (i.e., quartiles) may be comparable between congruent and incongruent trials, which would point to an independent modulation of conflict- and RT-related processes (Fig. 4, third panel). Alternatively, the slopes may differ between congruent and incongruent trials (e.g., steeper for incongruent trials), which would indicate that conflict- and RT-related processes determine MFC theta power interactively (Fig. 4, fourth panel).

To directly test these four alternatives, we sorted the stimulus-locked MFC theta power time courses in all trials by RT for each participant individually (Fig. 5C), and split the trials into four subsets representing different levels of response speed: fastest (mean RT: 526 ms), faster (mean RT: 593 ms), slower (mean RT: 650 ms), and slowest (mean RT: 733 ms). Each subset consisted of comparable numbers of trials (fastest: 221±32; faster: 221±22; slower: 225±32; slowest: 224±31; see Fig. 5D), with RT quartiles being computed across congruency conditions (i.e., each RT quartile corresponds to the same bounds for congruent and incongruent trials). This binning procedure resulted in the following trial allocations: on average, the bin of *fastest* RTs consisted of 160 congruent (mean RT: 524 ms) and 61 incongruent trials (mean RT: 532 ms); the *faster* bin of 121 congruent (mean RT: 591 ms) and 100 incongruent trials (mean RT: 595 ms); the *slower* bin of 94 congruent (mean RT: 649 ms) and 131 incongruent trials (mean RT: 651 ms); and the *slowest* bin of 86 congruent (mean RT: 729 ms) and 138 incongruent trials (mean RT: 734 ms).

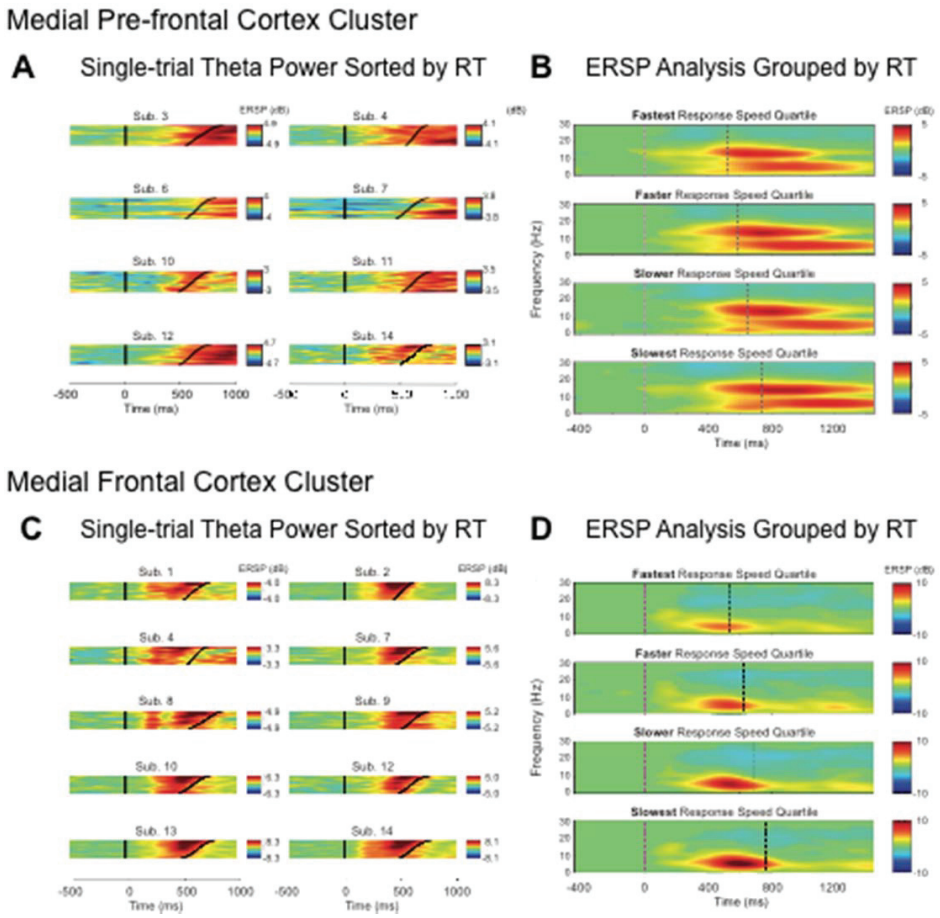

Figure 5. Fm theta power changes across congruent and incongruent trials sorted by RT and synchronized to stimulus onsets (at time 0). **A**, Spectrographic images of all trials sorted by RT for each of the 8 participants contributing to the MPFC cluster. **B**, MPFC ERSPs for trials in four RT-sorted groups (fastest, faster, slower, slowest). **C**, Spectrographic images of all trials sorted by RT for each of the 10 participants contributing to the MFC cluster. Note the higher mean theta power before slower responses (top traces in each panel) **D**, MFC ERSPs for trials in four RT-sorted groups (very fast, fast, slow, very slow). Note, again, that the theta power increase is larger in slower RT trials.

For each of the eight conditions, we then extracted theta-band ERSP values from the 200-ms time window ending at the mean trial-subset RT, and subjected them to repeated-measures ANOVAs with the factors 'S–R congruency' (congruent, incongruent) and 'Response speed'

(fastest, faster, slower, slowest). This ANOVA on mean changes in theta (4–7-Hz) log power revealed significant main effects of 'S–R congruency' and 'Response speed'. As shown in Figure 6C, weakest MFC theta bursts were elicited in trials with fastest RTs, with theta burst power gradually increasing as RTs became slower ($F(3,27) = 33.35$, $p < 0.01$). Independent of this response speed effect (interaction: $F(3,27) = 0.14$, $p > 0.94$), stimuli requiring spatially incongruent responses induced stronger MFC theta power than stimuli with spatially congruent responses ($F(1,9) = 14.85$, $p < 0.01$). This pattern indicates that conflict- and RT-related processes affect mean MFC theta power independently of one another (cf. Fig. 6D).

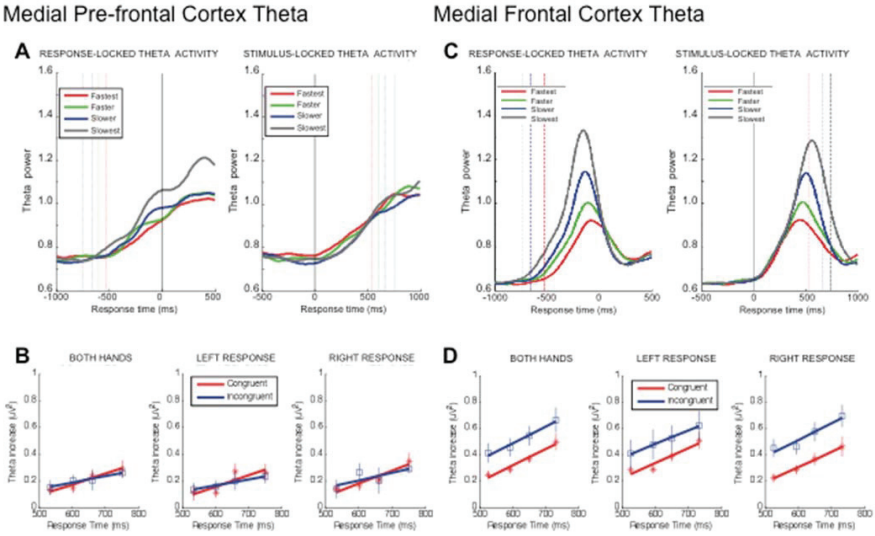

Figure 6. FM theta activity separately for each response speed quartile (fastest, faster, slower, slowest). **A**, RT quartile-dependent MPFC theta power synchronized to response (left panel) and stimulus onset (right panel). **B**, MPFC theta power separately for congruent (red) and incongruent trials (blue) as a function of RT quartile. **C**, RT quartile-dependent MFC theta power synchronized to response (left panel) and stimulus onset (right panel). **D**, MFC theta power separately for congruent (red) and incongruent trials (blue) as a function of RT quartile. Theta power was extracted from the 200-ms time window ending at the mean trial-subset RT, with theta increases estimated by subtracting mean baseline power in the (-1000-ms to -750-ms) time window before response onset.

While the interaction between 'S–R congruency' and 'Response speed' was far from significance ($p > 0.94$), it remains possible that the use of only four response speed bins was insufficient for the interaction to reach significance. For example, it may well be that variance becomes larger as RT increases, with a lot of important variance being lost when using RT quartiles. To control for this possibility, and to take the variance over all trials into account, we additionally computed within-subject correlations between MFC theta power and RTs, and then compared (Pearson's linear) correlation coefficients between congruent and incongruent conditions (using paired t-tests). This analysis revealed the difference between congruent (mean correlation coefficient: 0.18) and incongruent trials (mean correlation coefficient: 0.17) to be far from significance ($p > 0.85$), confirming the previous observation of MFC theta power being modulated independently by conflict- and RT-related processes in the present task.

Estimating relative contributions of conflict-related and -unrelated processes to MFC theta

In the next step, we attempted to estimate the relative contributions of conflict-related versus -unrelated processes to the increase in MFC theta power, that is: do the former make a greater, a smaller, or an equal contribution compared to the latter?

First, to estimate the *combined effects* of both conflict-related and -unrelated processes, we calculated the mean magnitude of the MFC theta increase across trials (in the 200-ms pre-response window of the respective ERSPs) *separately* for the congruent and incongruent conditions. For each RT bin (quartile), we multiplied the theta power value by the number of trials contained in the trial bin. The products of all four bins were then summed and subsequently divided by the total number of (congruent and, respectively, incongruent) trials. The difference between the resulting congruent- and incongruent-trial theta power was taken to reflect the *combined effects* of conflict- and RT-related processes on MFC theta power (Fig. 7D, left panel). Averaged across both hands, the overall difference between congruent and

incongruent trials was 0.22 μV^2 (*paired t-test*: $p < 0.005$). Looking at response side separately, the difference was more pronounced and significant for right-hand trials (0.28 μV^2; $p < 0.001$), and approached significance for left-hand trials (0.16 μV^2; $p < 0.06$).

Second, to isolate the "*conflict effect"* on MFC theta bursts from conflict-unrelated processes, we estimated the mean magnitude of the MFC theta increase across the RT quartiles (*separately* for the congruent and incongruent conditions). In detail, we summed theta power across all four RT bins and subsequently divided the sum by four (the number of bins). The difference—obtained by subtracting the resulting congruent from incongruent theta power (Fig. 7D, middle panel)—provides an estimate of the pure conflict-driven MFC theta increase. For both hands averaged, the (conflict-related) difference was significant (*paired t-test*: $p < 0.004$) and amounted to 0.17 μV^2, that is, 76% of the combined effect. As before, the difference was marginally larger for right-hand (0.21 μV^2; $p < 0.001$) than for left-hand trials (0.14 μV^2; $p < 0.07$).

Third, we estimated the contribution of "*conflict-unrelated processes"* to the MFC theta increase via averaging congruent and incongruent trials, thus effectively cancelling out (the contribution of) S–R conflicts. In detail, we calculated the theta power increase for each RT bin (*separately* for congruent and incongruent trials), taking the differential trial numbers per condition into account. That is, for each quartile, the theta power obtained (by averaging congruent and incongruent trials) was multiplied by the number of (congruent and, respectively, incongruent) trials contained in the respective bin. The products for all four bins were then summed up and subsequently divided by the total number of (congruent and incongruent) trials. As before, the difference—obtained by subtracting congruent from incongruent theta power (Fig. 7D, right panel)—provides and estimate of the pure contribution of *conflict-unrelated* processes to the MFC theta power increases. Across both response hands, there was a significant difference (*paired t-test*: $p < 0.01$) of 0.05 μV^2 (i.e., 24 % of the combined effect). Mirroring the previous analyses, the difference was stronger and

significant for right-hand trials (0.07 μV^2; $p < 0.001$), and approached significance level for left-hand trials (0.02 μV^2; $p < 0.07$).

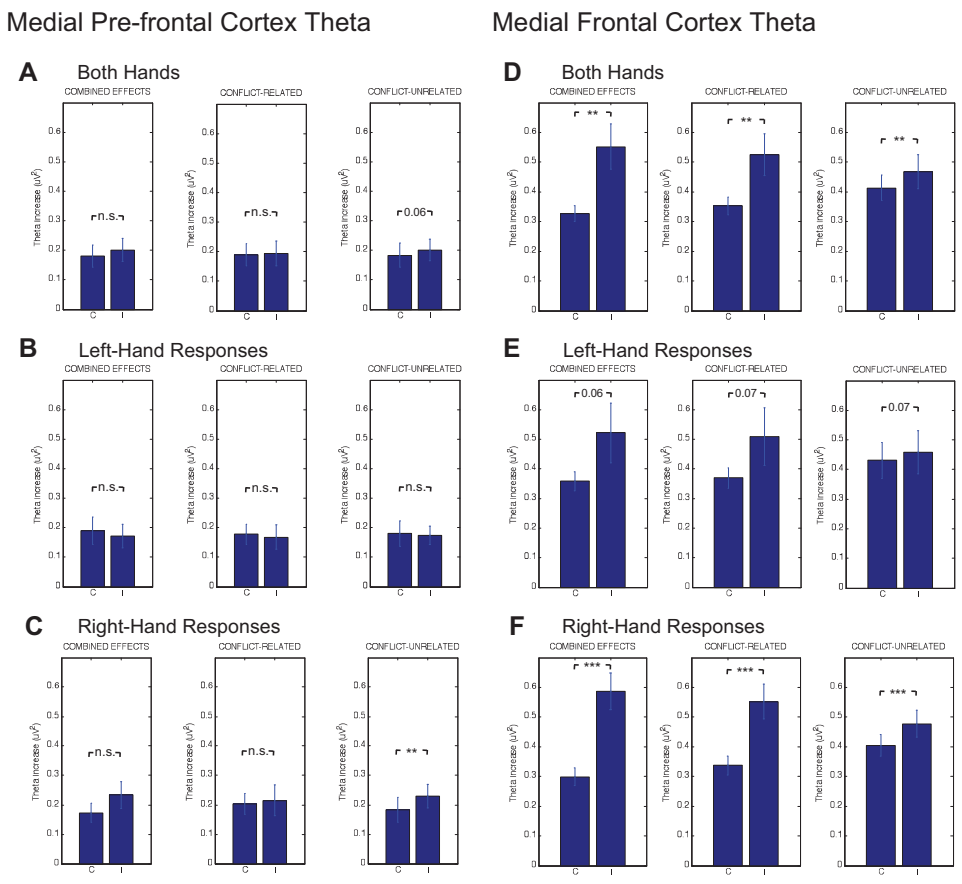

Figure 7. Fm theta activity (averaging ERSP values in the 200-msec window preceding the motor response) separately for congruent (C) and incongruent (I) trials. **A**, MPFC theta averaged across hands. **B**, MPFC theta for left-hand responses. **C**, MPFC theta for right-hand responses. **D**, MFC theta averaged across hands. **E**, MFC theta for left-hand responses. **F**, MFC theta for right-hand responses. Panels on the left in each sub-figure: C-I differences reflecting the "combined effects" of conflict and RT-related processes; central panels: C-I differences reflecting the isolated conflict effects; panels on the right: C-I differences reflecting the isolated effect of conflict-unrelated processes. Significant and non-significant differences between congruent and incongruent conditions are indicated by the respective p-values.

Response speed and MPFC theta

Although the previous analyses had revealed that the present MPFC theta complex was elicited independently of S–R conflict, it cannot no be ruled out that this complex indexes S–R conflicts for a subset of trials (e.g., in slower but not in faster RT quartiles)—a pattern that might have remained hidden when performing the analyses for congruent and incongruent conditions averaged across all trials. To control for this possibility, we performed the same RT quartile-dependent analyses for the MPFC theta power as (described above) for the MFC theta power. Stimulus-locked MPFC theta power time courses in all trials were first sorted by RT for each participant individually (Fig. 5A) and then divided into four quartile bins representing different response speed levels (Fig. 5B). Theta-band ERSP values from the 200-ms time window ending at the mean trial-subset RT, extracted separately for each of the eight conditions, were used for statistical comparisons. Of note, the different RT quartiles consisted of exactly the same (congruent and incongruent) trials as the MFC theta power analyses.

The repeated-measures ANOVA with the factors 'S–R congruency' (congruent, incongruent) and 'Response speed' (fastest, faster, slower, slowest) on MPFC theta (4-7 Hz) log power revealed the main effect of 'Response speed' to be significant ($F(3,21) = 8.80$, $p < 0.01$), whereas the main effect of 'S–R congruency' ($F(1,7) = 0.04$, $p > 0.83$) and the interaction ($F(3,21) = 0.97$, $p > 0.42$) were non-significant. As depicted in Figure 6B, the response speed effect is due to generally increasing MPFC theta power for trials with slower relative to faster RTs, without an effect of or modulation by S–R congruency. As for the MFC analyses, we also computed within-subject correlations between MPFC theta power and RTs (for comparisons of correlation coefficients between congruent and incongruent conditions) to examine whether the non-significant interaction might be due to variance loss owing to our RT binning procedure (see above). Supporting our previous findings, this analysis confirmed that RT-related processes modulated MPFC theta power independently of S-R congruence—as evidenced by statistically indifferent ($p > 0.65$) mean correlation coefficients for congruent

(0.08) and incongruent trials (0.07). Given that response speed modulated both MPFC and MFC theta power, we further examined whether the effect of RT on the two clusters correlate with one another. These analyses revealed a significant correlation for congruent trials ($p < 0.05$), but not for incongruent trials ($p > 0.19$)—corroborating that conflict-unrelated effects in fmθ power are not selective to the MFC complex.

Quantifying the contribution of RT-related processes to MPFC theta

Finally, we sought to quantify the contribution of conflict-unrelated processes to the MPFC theta bursts triggered in congruent and incongruent trials, and to assess whether the RT-related influence depends on (left versus right) response side. To this end, we performed the same analysis for the MPFC power as used for estimating the relative contributions of conflict-related and -unrelated processes to the MFC theta power (see above).

For the *conflict-unrelated* influence to MPFC theta power, we found a significant difference between congruent and incongruent trials for right-hand (0.05 μV^2; *paired t-test*: $p < 0.01$; Fig. 7C), but not for left-hand (-0.01 μV^2; *paired t-test*: $p > 0.73$; Fig. 7B) responses. When averaged across hands, the difference between congruent and incongruent trials was only marginally significant (*paired t-test*: $p < 0.06$), amounting to 0.02 μV^2. To provide a full picture of the present MPFC theta complex, we also estimated the contribution of putative conflict-related differences to MPFC theta power (using the RT quartile-dependent procedure as described above), and examined whether congruent and incongruent trials remained statistically different when computing the *combined effects*, which represent essentially the sum of conflict-unrelated and (putatively present) conflict-related differences across S–R conditions. Consistent with our previous findings, this analysis showed that MPFC theta bursts during congruent and incongruent trials were triggered independently of S–R conflict (all p-values: > 0.43). Similarly, none of the comparisons reached statistical significance for the combined effects (all p-values: > 0.15).

Discussion

In the current study, we set out to explore whether there are several theta generators in or near anterior cingulate cortex that jointly give rise to the scalp-recorded EEG spectral responses typically found in paradigms involving S–R conflicts (Nigbur et al., 2011; Cavanagh et al., 2012; van Driel et al., 2012). In particular, we aimed at identifying the cortical areas generating conflict-induced fmθ complexes in a Simon-type manual reaching task to resolve the open issue whether multiple, conflict-related (detection and adaptation) and conflict-unrelated processes (general RT slowing) can be linked to statistically independent fmθ oscillations; or, alternatively, whether multiple processes can drive one-and-the-same fmθ complex. At the behavioral level, our results replicated the pattern well-known from the Simon task literature (Simon, 1969; Hommel, 1995): participants' RTs were slower for incongruent than for congruent trials, with the incongruency effect being reduced on trials that followed a conflict on the previous trial.

Two independent fmθ generators

By means of ICA decomposition (Makeig et al., 1996), our EEG analyses identified two functionally distinct fmθ patterns during target processing, both of which started around 400 ms post-stimulus and exhibited a clear fmθ-related scalp distribution. Dipole source localization revealed that one fmθ oscillation was triggered in (or near) the MFC, while the other originated from a more anterior region of medial cortex: the MPFC. The most important observation was, however, that only the former cluster reflected the non-correspondence (i.e., the conflict) between S and R locations. In particular, MFC theta power was enhanced for incongruent relative to congruent trials, whereas no such difference was discernable for MPFC theta power. Moreover, MFC theta activity was modulated by trial-to-trial (conflict) history—with reduced MFC theta power triggered in incongruent trials when participants had

processed a conflict on the trial before—and depended additionally on conflict-*unrelated* processes that were associated with RT slowing.

The finding that spatially incongruent S–R situations give rise to a stronger fmθ response that is modulated by trial-to-trial history is in accord with recent studies that used classical (Cohen and Ridderinkhof, 2013; Gulbinaite et al., 2014) or diverse (cueing) versions of the Simon task (Cavanagh et al., 2012; van Driel et al., 2015). From all these studies, however, it remained unclear (i) whether this pattern originates from a mixture of multiple fmθ sources in the MFC, and, if so, (ii) whether they are all related to conflict detection and/or subject to trial-to-trial adaptation. Thus, to our knowledge, our findings provide the first demonstration that at least two classes of functionally independent fmθ generators are simultaneously active during conflict processing in a Simon-type task. Critically, only one of the two produced larger theta responses in trials with S–R incongruency, providing strong electrophysiological support for the recent proposal that a single, spatially restricted microcircuit in the MFC is responsible for the detection and signaling of conflict (Cohen, 2014).

Dissociating conflict from conflict-unrelated processes in MFC theta oscillations

Our results yield important insights for a challenge that can be leveled against virtually all studies using RT paradigms to explore EEG oscillations, namely, that the change in the oscillatory pattern may be a direct correlate of a concurrent RT change. In this regard, it has been argued that the increase in theta activity for incongruent relative to congruent trials, rather than reflecting the S–R conflict *per se*, may be an effect of increased RTs or more general, conflict-independent RT-slowing processes (Scherbaum and Dshemuchadse, 2013). Arguing against this view, opponents pointed out that this notion has limitations when taking neurobiological and psychological constraints into account (Cohen and Nigbur, 2013)—favoring the view that fmθ tracks the strength of response conflict and that RT can be taken as a behavioral index of such a conflict.

Here we show that conflict-related MFC theta bursts in a Simon-type task cannot be attributed to a single factor: MFC theta was larger in trials on which S–R locations differed and, independently of this conflict-related modulation, increased in trials with slower responses. This pattern is consistent with the compromise view that MFC theta increases in the present task are determined both by conflict-related and general RT-slowing processes. Specifically, processes not related to conflict contributed approximately one quarter to the overall MFC theta bursts (averaged across both hands; Fig. 7D), with conflict-related processes contributing the 'lion's share' (approximately three quarters). Concerning the former, potential candidates for RT slowing processes that are not related to conflict include attentional resource allocation during visuo-motor processing (Makeig et al., 2004; Sauseng et al., 2007; Cravo et al., 2011), decision-making (Rushworth et al., 2004; Womelsdorf et al., 2010; Euston et al., 2012), or working memory-related processes (Gevins et al., 1997; Jensen and Tesche, 2002; Onton et al., 2005). However, to what degree each of these, or alternative, conflict-unrelated factors may have contributed to the present MFC theta power remains an open issue (to be resolved in future studies).

Conflict-induced fmθ complexes as a common neural substrate for cognitive control in response-override tasks?

Finally, there has been a steadily growing interest in fmθ and the idea that conflict-related characteristics of this brain response may reflect a *unitary* cognitive control mechanism for human conflict processing (Ridderinkhof et al., 2004; Nigbur et al., 2011; Cavanagh and Frank, 2014). For example, it has been proposed that non-phase-locked theta induced by conflicting task information modulates obligatory phase-locked theta responses evoked by perceptual and/or action events, resulting in the well-established pattern of conflict-related fmθ increases (Cohen and Donner, 2013). Support for this notion derived from recent electrocortical findings from a particular class of conflict tasks that, as the Simon task, is

619 characterized by a competition between the appropriate response demanded by the stimulus
620 and an alternative, pre-potent response that has to be overridden. Other examples of such
621 response-override tasks include the Stroop task (Hanslmayr et al., 2008; Oehrn et al., 2014),
622 the Eriksen flanker task (Cavanagh et al., 2009; Nigbur et al., 2012), and the response-priming
623 task (Pastötter et al., 2010; Pastötter et al., 2013). Hanslmayr and colleagues (2008), for
624 instance, observed stronger scalp fmθ responses for incongruent relative to congruent stimuli
625 in the Stroop task. Essentially the same pattern has been replicated for the Eriksen flanker task
626 (Nigbur et al., 2012) and the response-priming task (Pastötter et al., 2013). Given these
627 similarities, there is a general consensus that the same cognitive control process, indexed by
628 conflict-induced fmθ complexes, may mediate interference detection and conflict monitoring
629 across response-override tasks.

630 While there is undoubtedly a remarkable overlap across various conflict paradigms (Lu
631 and Proctor, 1995) and beyond (Rushworth et al., 2007), it remains a point of contention
632 whether conflict-related fmθ increases reflect indeed the *very same* cognitive control
633 mechanism. Put differently, if conflict-induced fmθ complexes represent a *unitary, task-*
634 *independent* process for detecting and resolving conflicts across response-override tasks, then
635 one would predict that, irrespective of the specific task at hand, this brain response should be
636 (i) generated in *exactly* the same cortical region, and (ii) *similarly* sensitive to inter-trial
637 (conflict) history. Closer inspection of the recent response-override task literature discloses,
638 however, that these criteria are not fulfilled. First, it has been shown that, even though
639 incongruent relative to congruent trial types give rise to a brief increase in theta EEG power
640 with a clear focus over fmθ areas in the Stroop, Simon, and response-priming tasks, their
641 exact underlying neural sources vary. Whereas conflict-related fmθ elicited in response-
642 priming tasks originates from the left ACC, extending to the left pre-SMA (Pastötter et al.,
643 2013), the sources generating conflict-related fmθ in the Stroop task (Hanslmayr et al., 2008)

644 and the present Simon-type task were localized, without any consistent lateralization to one
645 cerebral hemisphere, in the dorsal ACC. Moreover, while conflict-related fmθ power in both
646 the response-priming task (Pastötter et al., 2013) and the present Simon-type task were
647 influenced by conflicts on the previous trial, no such adaptation effects have been found for
648 trial-averaged theta responses in the Erikson task (Cohen and Cavanagh, 2011).

649 Thus, despite striking similarities of fmθ across various response-override tasks, there are
650 also crucial differences that mitigate the hypothesis of conflict-related fmθ as reflecting the
651 *very same* cognitive control mechanism for resolving conflict. Notably, the pattern of task-
652 dependent, conflict-related fmθ increases provides electrocortical evidence for the view, put
653 forward by Hommel (2011), that the Simon, Stroop, and Erikson effects should not be treated
654 as representing the same (conflict) phenomena. As pointed out by Hommel (2011), the Simon
655 effect can be traced back to the non-correspondence between S–R locations. For the Erikson
656 and Stroop effects, by contrast, the conflict-induced response slowing may have at least two
657 sources: any cost for incongruent trials in these tasks may be due to the conflict between the
658 two stimulus-related feature codes (e.g., blue vs. red colors and, respectively, target vs.
659 flanker items), the conflict between the associated response codes, or a mixture of both. Taken
660 together, our results fit well with the notion of task-dependent brain processes that resolve
661 experienced stimulus-stimulus and stimulus-response conflicts across different response-
662 override tasks and which likely translate into task-dependent fmθ characteristics.

663

664 **Acknowledgements**

665 The authors would like to thank Mike X. Cohen and two anonymous reviewers for their
666 helpful comments on an earlier version of this manuscript. The authors are grateful to Andre
667 Vankov for technical assistance, and gratefully acknowledge to SM the gift from The Swartz
668 Foundation (Old Field, NY) that made possible our collaboration.

669

References

Bell AJ, Sejnowski TJ (1995) An information-maximization approach to blind separation and blind deconvolution. Neural computation 7:1129-1159.

Botvinick MM, Cohen JD, Carter CS (2004) Conflict monitoring and anterior cingulate cortex: an update. Trends in cognitive sciences 8:539-546.

Buzsaki G (2006) Rhythms of the Brain: Oxford University Press.

Cavanagh JF, Frank MJ (2014) Frontal theta as a mechanism for cognitive control. Trends in cognitive sciences 18:414-421.

Cavanagh JF, Cohen MX, Allen JJ (2009) Prelude to and resolution of an error: EEG phase synchrony reveals cognitive control dynamics during action monitoring. The Journal of Neuroscience 29:98-105.

Cavanagh JF, Zambrano-Vazquez L, Allen JJ (2012) Theta lingua franca: A common mid-frontal substrate for action monitoring processes. Psychophysiology 49:220-238.

Cohen MX (2014) A neural microcircuit for cognitive conflict detection and signaling. Trends in neurosciences 37:480-490.

Cohen MX, Cavanagh JF (2011) Single-trial regression elucidates the role of prefrontal theta oscillations in response conflict. Frontiers in psychology 2:30.

Cohen MX, Donner TH (2013) Midfrontal conflict-related theta-band power reflects neural oscillations that predict behavior. Journal of Neurophysiology 110:2752-2763.

Cohen MX, Nigbur R (2013) Reply to "Higher response time increases theta energy, conflict increases response time". Clinical Neurophysiology 124:1479-1481.

Cohen MX, Ridderinkhof KR (2013) EEG source reconstruction reveals frontal-parietal dynamics of spatial conflict processing. PLoS One 8:e57293.

Cohen MX, Ridderinkhof KR, Haupt S, Elger CE, Fell J (2008) Medial frontal cortex and response conflict: evidence from human intracranial EEG and medial frontal cortex lesion. Brain research 1238:127-142.

Cravo AM, Rohenkohl G, Wyart V, Nobre AC (2011) Endogenous modulation of low frequency oscillations by temporal expectations. Journal of neurophysiology 106:2964-2972.

Delorme A, Makeig S (2004) EEGLAB: an open source toolbox for analysis of single-trial EEG dynamics including independent component analysis. Journal of neuroscience methods 134:9-21.

Delorme A, Palmer J, Onton J, Oostenveld R, Makeig S (2012) Independent EEG sources are dipolar. PloS one 7:e30135.

Egner T (2007) Congruency sequence effects and cognitive control. Cognitive, Affective, & Behavioral Neuroscience 7:380-390.

Euston DR, Gruber AJ, McNaughton BL (2012) The role of medial prefrontal cortex in memory and decision making. Neuron 76:1057-1070.

Fuchs M, Kastner J, Wagner M, Hawes S, Ebersole JS (2002) A standardized boundary element method volume conductor model. Clinical Neurophysiology 113:702-712.

Gevins A, Smith ME, McEvoy L, Yu D (1997) High-resolution EEG mapping of cortical activation related to working memory: effects of task difficulty, type of processing, and practice. Cerebral cortex 7:374-385.

Gramann K, Onton J, Riccobon D, Mueller HJ, Bardins S, Makeig S (2010) Human brain dynamics accompanying use of egocentric and allocentric reference frames during navigation. Journal of cognitive neuroscience 22:2836-2849.

Gratton G, Coles MG, Donchin E (1992) Optimizing the use of information: strategic control of activation of responses. Journal of Experimental Psychology: General 121:480.

Gulbinaite R, van Rijn H, Cohen MX (2014) Fronto-parietal network oscillations reveal relationship between working memory capacity and cognitive control. Frontiers in human neuroscience 8:761.

Hanslmayr S, Pastötter B, Bäuml K-H, Gruber S, Wimber M, Klimesch W (2008) The electrophysiological dynamics of interference during the Stroop task. Journal of Cognitive Neuroscience 20:215-225.

Hommel B (1995) Stimulus-response compatibility and the Simon effect: Toward an empirical clarification. Journal of Experimental Psychology: Human Perception and Performance 21:764.

Hommel B (2011) The Simon effect as tool and heuristic. Acta Psychologica 136:189-202.

Hommel B, Proctor RW, Vu K-PL (2004) A feature-integration account of sequential effects in the Simon task. Psychological research 68:1-17.

Ishii R, Shinosaki K, Ukai S, Inouye T, Ishihara T, Yoshimine T, Hirabuki N, Asada H, Kihara T, Robinson SE (1999) Medial prefrontal cortex generates frontal midline theta rhythm. Neuroreport 10:675-679.

Jensen O, Tesche CD (2002) Frontal theta activity in humans increases with memory load in a working memory task. European journal of Neuroscience 15:1395-1399.

Kerns JG (2006) Anterior cingulate and prefrontal cortex activity in an FMRI study of trial-to-trial adjustments on the Simon task. Neuroimage 33:399-405.

729 Lee T-W, Girolami M, Sejnowski TJ (1999) Independent component analysis using an extended infomax
730 algorithm for mixed subgaussian and supergaussian sources. Neural computation 11:417-441.
731 Lewicki MS, Sejnowski TJ (2000) Learning overcomplete representations. Neural computation 12:337-365.
732 Lu C-H, Proctor RW (1995) The influence of irrelevant location information on performance: A review of the
733 Simon and spatial Stroop effects. Psychonomic bulletin & review 2:174-207.
734 Makeig S (1993) Auditory event-related dynamics of the EEG spectrum and effects of exposure to tones.
735 Electroencephalography and clinical neurophysiology 86:283-293.
736 Makeig S, Bell AJ, Jung T-P, Sejnowski TJ (1996) Independent component analysis of electroencephalographic
737 data. Advances in neural information processing systems:145-151.
738 Makeig S, Westerfield M, Jung T-P, Enghoff S, Townsend J, Courchesne E, Sejnowski TJ (2002) Dynamic brain
739 sources of visual evoked responses. Science 295:690-694.
740 Makeig S, Delorme A, Westerfield M, Jung T-P, Townsend J, Courchesne E, Sejnowski TJ (2004)
741 Electroencephalographic brain dynamics following manually responded visual targets. PLoS Biol
742 2:e176.
743 Mayr U, Awh E, Laurey P (2003) Conflict adaptation effects in the absence of executive control. Nature
744 neuroscience 6:450-452.
745 Mückschel M, Stock A-K, Dippel G, Chmielewski W, Beste C (2016) Interacting sources of interference during
746 sensorimotor integration processes. Neuroimage 125:342-349.
747 Nigbur R, Ivanova G, Stürmer B (2011) Theta power as a marker for cognitive interference. Clinical
748 Neurophysiology 122:2185-2194.
749 Nigbur R, Cohen MX, Ridderinkhof KR, Stürmer B (2012) Theta dynamics reveal domain-specific control over
750 stimulus and response conflict. Journal of Cognitive Neuroscience 24:1264-1274.
751 Oehrn CR, Hanslmayr S, Fell J, Deuker L, Kremers NA, Do Lam AT, Elger CE, Axmacher N (2014) Neural
752 communication patterns underlying conflict detection, resolution, and adaptation. The Journal of
753 Neuroscience 34:10438-10452.
754 Onton J, Delorme A, Makeig S (2005) Frontal midline EEG dynamics during working memory. Neuroimage
755 27:341-356.
756 Oostenveld R, Oostendorp TF (2002) Validating the boundary element method for forward and inverse EEG
757 computations in the presence of a hole in the skull. Human brain mapping 17:179-192.
758 Palmer JA, Kreutz-Delgado K, Makeig S (2006) Super-Gaussian mixture source model for ICA. In: International
759 Conference on Independent Component Analysis and Signal Separation, pp 854-861: Springer.
760 Palmer JA, Makeig S, Kreutz-Delgado K, Rao BD (2008) Newton method for the ICA mixture model. In:
761 Icassp, pp 1805-1808.
762 Pastötter B, Hanslmayr S, Bäuml K-HT (2010) Conflict processing in the anterior cingulate cortex constrains
763 response priming. Neuroimage 50:1599-1605.
764 Pastötter B, Dreisbach G, Bäuml K-HT (2013) Dynamic adjustments of cognitive control: oscillatory correlates
765 of the conflict adaptation effect. Journal of cognitive neuroscience 25:2167-2178.
766 Ridderinkhof KR, Ullsperger M, Crone EA, Nieuwenhuis S (2004) The role of the medial frontal cortex in
767 cognitive control. science 306:443-447.
768 Rushworth M, Walton ME, Kennerley SW, Bannerman D (2004) Action sets and decisions in the medial frontal
769 cortex. Trends in cognitive sciences 8:410-417.
770 Rushworth MF, Buckley MJ, Behrens TE, Walton ME, Bannerman DM (2007) Functional organization of the
771 medial frontal cortex. Current opinion in neurobiology 17:220-227.
772 Sauseng P, Hoppe J, Klimesch W, Gerloff C, Hummel F (2007) Dissociation of sustained attention from central
773 executive functions: local activity and interregional connectivity in the theta range. European Journal of
774 Neuroscience 25:587-593.
775 Scherbaum S, Dshemuchadse M (2013) Higher response time increases theta energy, conflict increases response
776 time. Clinical Neurophysiology 124:1477-1479.
777 Simon JR (1969) Reactions toward the source of stimulation. Journal of experimental psychology 81:174.
778 Simon JR, Small Jr A (1969) Processing auditory information: interference from an irrelevant cue. Journal of
779 Applied Psychology 53:433.
780 Töllner T, Müller HJ, Zehetleitner M (2012a) Top-down dimensional weight set determines the capture of visual
781 attention: Evidence from the PCN component. Cerebral Cortex 22:1554-1563.
782 Töllner T, Rangelov D, Müller HJ (2012b) How the speed of motor-response decisions, but not focal-attentional
783 selection, differs as a function of task set and target prevalence. Proceedings of the National Academy
784 of Sciences 109:E1990-E1999.
785 Töllner T, Gramann K, Müller HJ, Kiss M, Eimer M (2008) Electrophysiological markers of visual dimension
786 changes and response changes. Journal of Experimental Psychology: Human Perception and
787 Performance 34:531.
788 Ullsperger M, Bylsma LM, Botvinick MM (2005) The conflict adaptation effect: It's not just priming. Cognitive,
789 Affective, & Behavioral Neuroscience 5:467-472.
790 Umiltà C, Nicoletti R (1992) An integrated model of the Simon effect.

van Driel J, Ridderinkhof KR, Cohen MX (2012) Not all errors are alike: theta and alpha EEG dynamics relate to differences in error-processing dynamics. The Journal of Neuroscience 32:16795-16806.

van Driel J, Swart JC, Egner T, Ridderinkhof KR, Cohen MX (2015) (No) time for control: Frontal theta dynamics reveal the cost of temporally guided conflict anticipation. Cognitive, Affective, & Behavioral Neuroscience 15:787-807.

Wallace RJ (1971) SR compatibility and the idea of a response code. Journal of experimental psychology 88:354.

Womelsdorf T, Vinck M, Leung SL, Everling S (2010) Selective theta-synchronization of choice-relevant information subserves goal-directed behavior. Frontiers in human neuroscience 4:210.

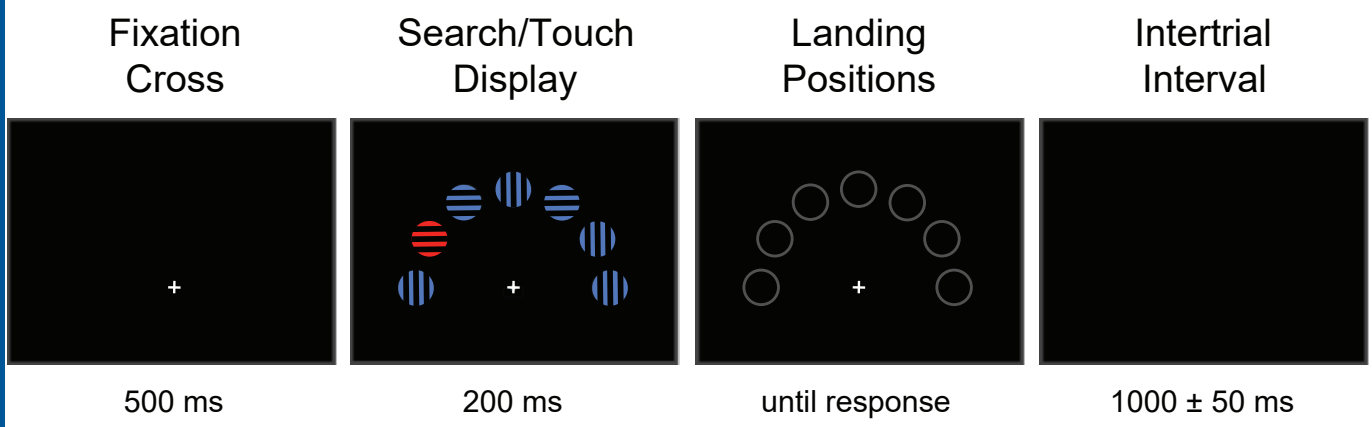

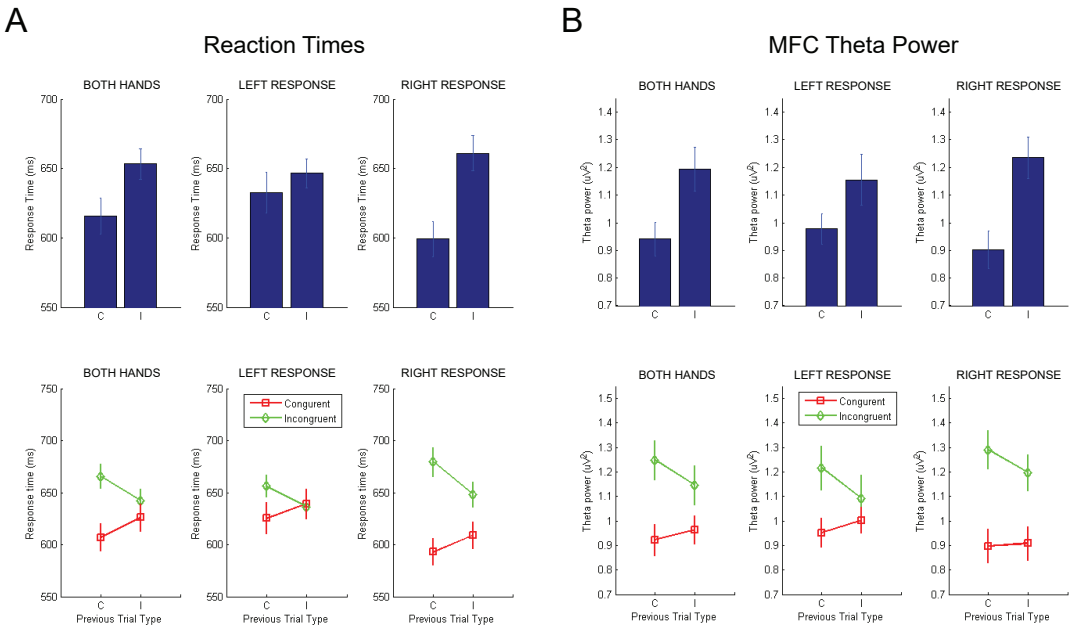

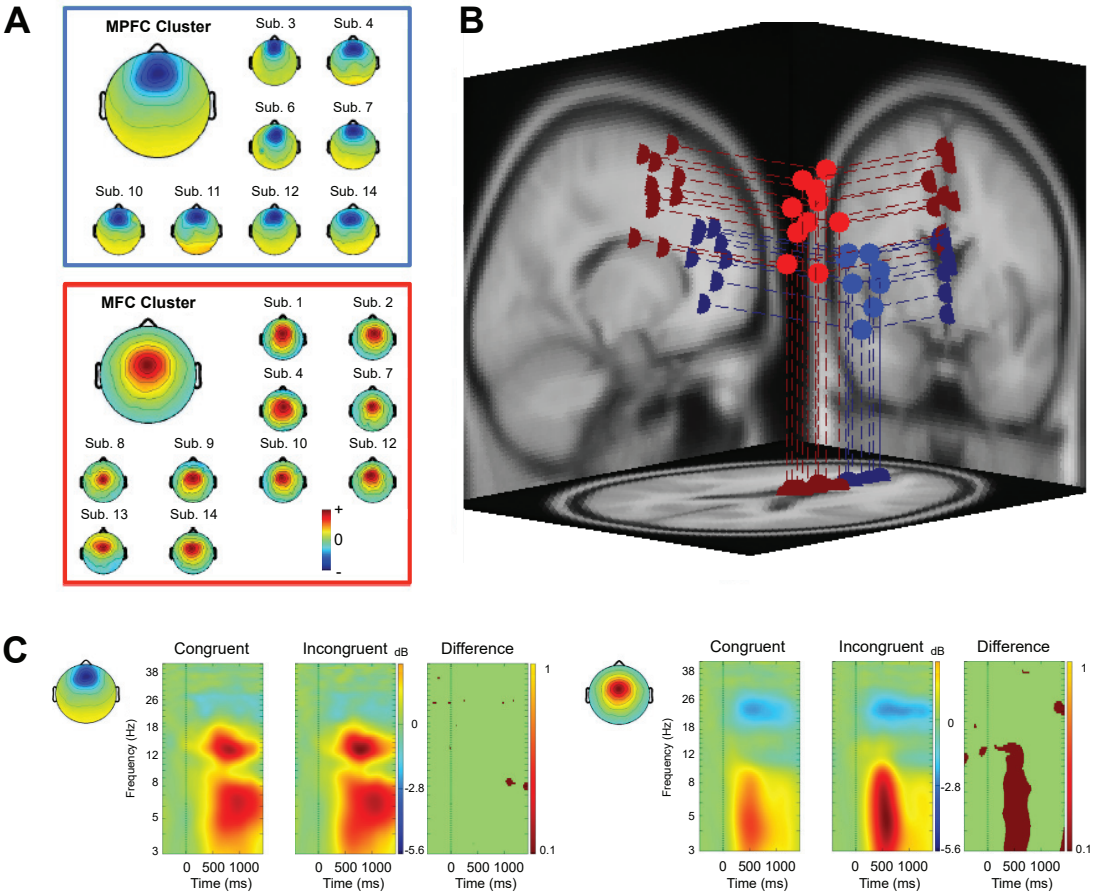

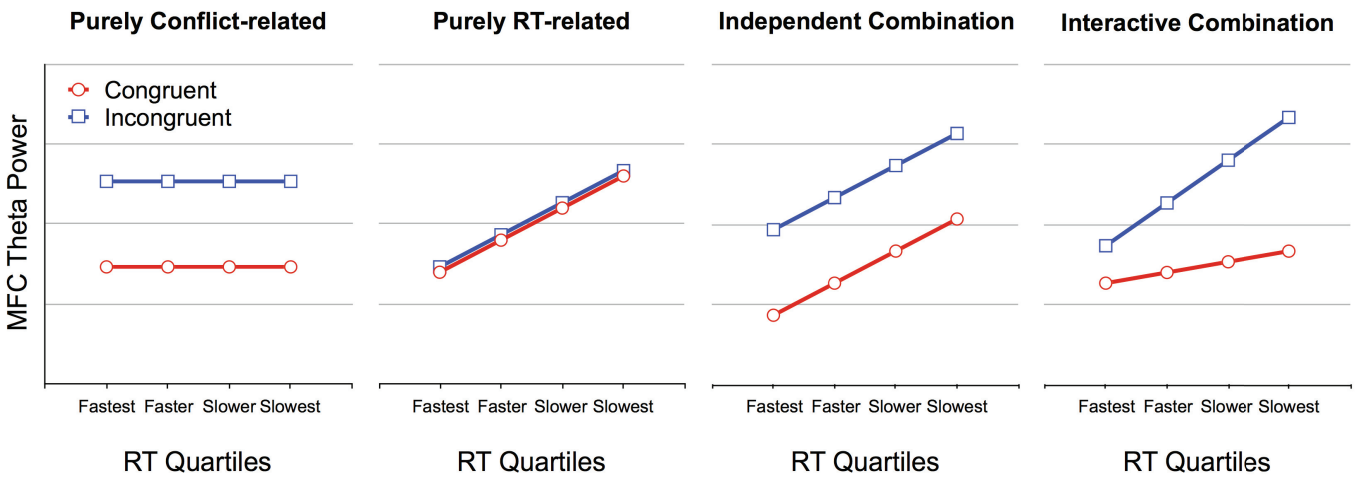

Medial Pre-frontal Cortex Cluster

A Single-trial Theta Power Sorted by RT

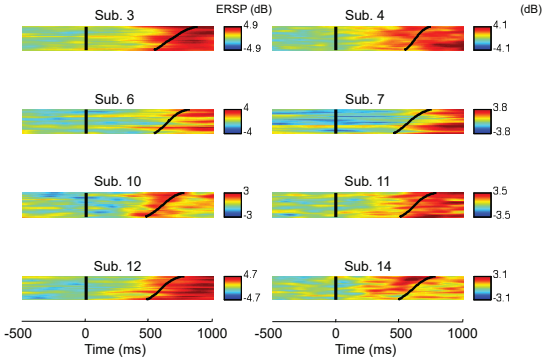

B ERSP Analysis Grouped by RT

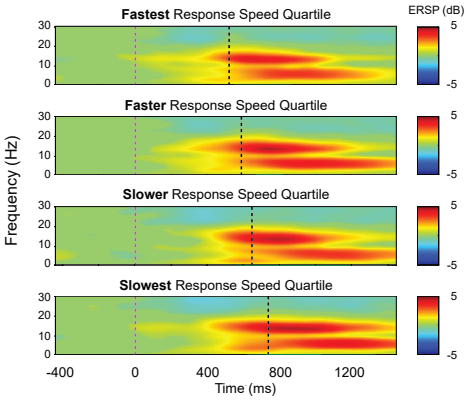

Medial Frontal Cortex Cluster

C Single-trial Theta Power Sorted by RT

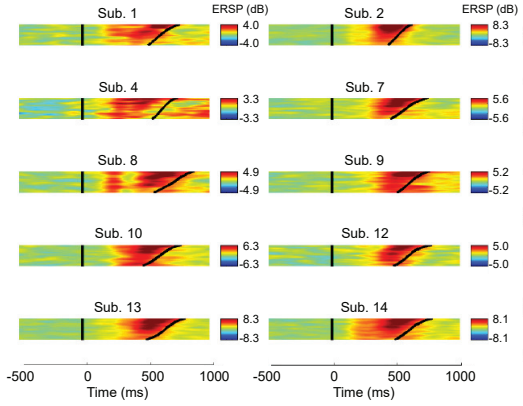

D ERSP Analysis Grouped by RT

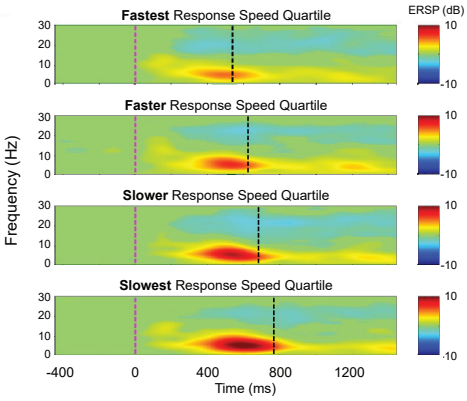

Medial Pre-frontal Cortex Theta

Medial Frontal Cortex Theta

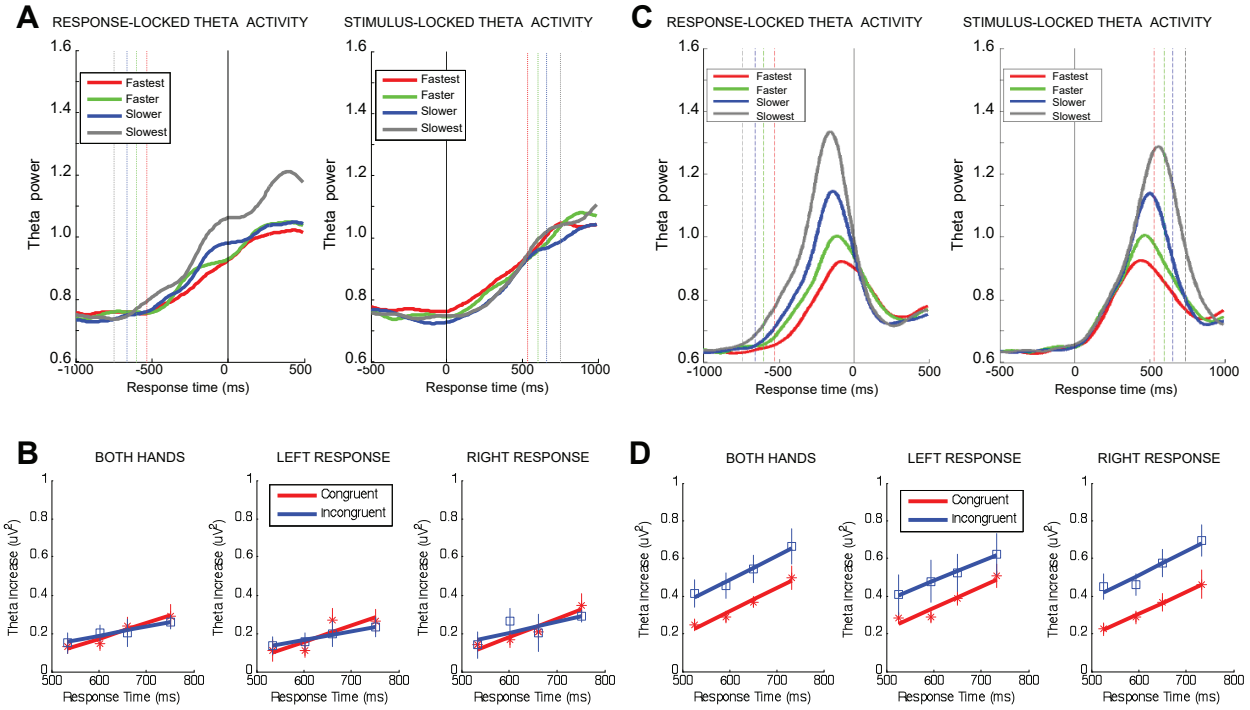

Medial Pre-frontal Cortex Theta

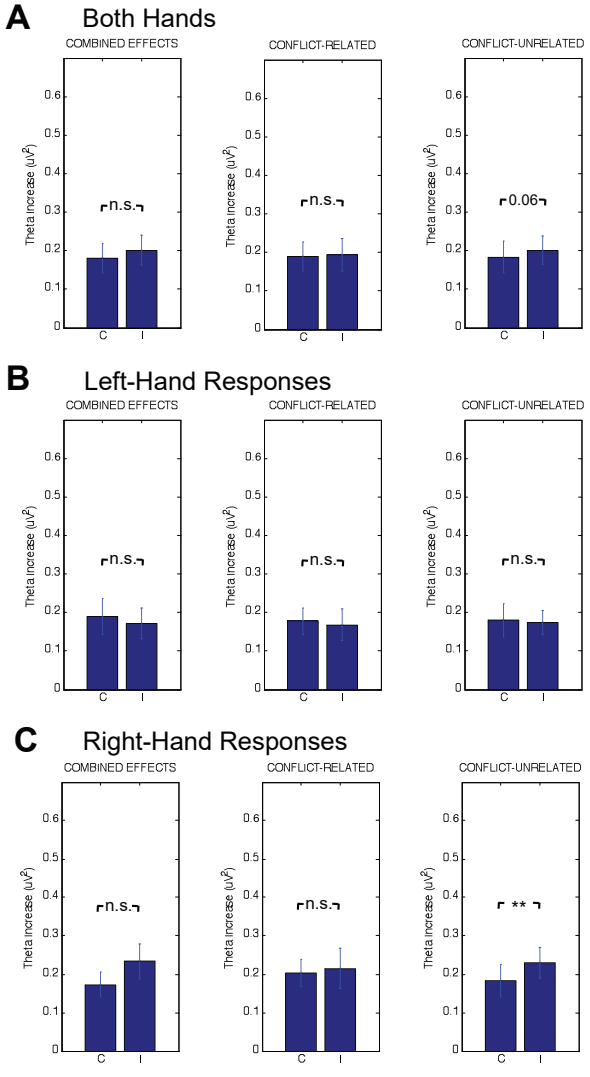

Medial Frontal Cortex Theta